Available online at http://scik.org
Commun. Math. Biol. Neurosci. 2025, 2025:101
https://doi.org/10.28919/cmbn/9401
ISSN: 2052-2541

COMPUTATIONAL OPTIMIZATION OF FRACTIONAL-ORDER INFLUENZA SIR EPIDEMIC MODELING USING TWO EFFECTIVE TECHNIQUES

FARIS MAHDI ALWAN[1], D. K. ARCHANA[2], D. G. PRAKASHA[2], ALI HASAN ALI[3,4,5,*]

[1]Department of Statistics, College of Administration and Economics, University of Baghdad, Baghdad, Iraq

[2]Department of Mathematics, Davangere University, Shivagangotri, Davangere - 577007, India

[3]Department of Mathematics, College of Education for Pure Sciences, University of Basrah, Basrah, Iraq

[4]Department of Business Management, Al-imam University College, 34011, Balad, Iraq

[5]Technical Engineering College, Al-Ayen University, 64001, Dhi Qar, Iraq

Abstract. In this study, we employ two efficient approaches, the $q-$homotopy analysis transform method and the Predictor-Corrector method to find and analyze the solution for the fractional order influenza SIR epidemic model. In recent times, numerous innovative definitions of fractional derivatives have been proposed and employed to construct mathematical models for an extensive array of complex problems, including nonlocal effects, memory, and history. We implement the Caputo fractional derivative for the considered SIR epidemic model of influenza which is characterized by ordinary differential equations of nonlinear form. The $q-$homotopy analysis method and the Laplace transform are combined to form the basis of $q-$homotopy analysis transform method. The outcomes of the methods under consideration can be found as a quickly convergent solutions. To illustrate the accuracy, speed, and high order of convergence of the $q-$homotopy analysis transform method, its solution is compared to that produced by the Residual power series method and fourth-order Runge-Kutta method. The 3D plots, graphs and numerical results express the physical representation of the considered model. It exhibits that the Predictor-Corrector approach and the $q-$homotopy analysis transform method are meticulous, reliable, and effective to examine the suggested influenza SIR epidemic model and a few other fractional order differential equations in

*Corresponding author

E-mail address: aliaha1@yahoo.com

Received June 4, 2025

epidemiology. The details of the solution behavior are provided by this analysis, which ensures accurate epidemic predictions. In addition to improving epidemic modeling, this new approach is a more precise tool for forecasting and planning public health. The paper establishes an evaluation for fractional epidemic models and demonstrates the utility of the methods in the context of disease transmission.

Keywords: caputo fractional derivative; influenza model; operations research; $q-$homotopy analysis transform method; laplace transform; predictor-corrector algorithm.

2020 AMS Subject Classification: 26A33, 34A08, 92D30.

1. INTRODUCTION

Comprehending infectious diseases and controlling them requires an grasp of epidemiology, which is the study of health-related events, the general health of communities and how frequently diseases occur in certain groups of people and why. Flu is also referred as influenza, which affecting millions of people annually and posing a serious risk to public health. Because it is seasonal, infectious, and can result in catastrophic sickness, flu poses a serious challenge to the integrity of global helath. Influenza viruses are respiratory illness that spread throughout populations and frequently result in large-scale outbreaks and epidemics. The World Health Organization (WHO) estimates that seasonal influenza epidemics cause between 290,000 and 645,000 respiratory fatalities and 3 to 5 million cases of severe illness annually around the world, indicating the substantial burden of seasonal influenza [1].

Fractional Calculus (FC) is a branch of mathematical analysis that deals with the investigation and understanding of fractional-order (FO) derivatives and integrals. It introduces an ability to use not only integer orders of differentiation and integration, but non-integer ones as well, and thus enables amplification of concepts that we learned in classical calculus. Fractional differential equations (FDEs) which involve fractional derivatives (FDs) are very powerful tools for modeling complex systems in physics, engineering, economics, biology, and other fields. The ability of FDEs to describe peculiar features and distant interactions in the systems makes them especially useful in describing memory driven, anomalous and nonlocal behaviours. FC has been the result of several eminent researchers as its definitions have gotten new directions. Miller and Ross [2] provide a comprehensive overview of FC and FDEs, detailing important terminology and approaches to solving them. It discusses examples from physics, engineering,

and biology, with a focus on memory effects and intrinsic properties. This and other aspects of FC are detailed in [3], covering the conceptual foundations, the analytical and numerical techniques, and the applications in control theory. Covering FDs, stability analysis, and solution methodologies, this is a much needed reference for applied mathematicians and engineers alike. M. Caputo proposed the Caputo fractional derivative (CFD) in order to generalize viscoelastic and dissipative systems [4]. The fractional and classical calculus are integrated through coupling memory effects and modeling materials [5]. FC has its roots in the early ideas of Leibniz, which have been formalized in [6] by B. Ross. The time period of seminal contributions, mathematical development and the slow climb of FDs provides insight into this branch of mathematics. FC has been widely used in a multitude of disciplines such as signal processing [7], financial markets [8], human disease [9], image processing [10], modeling of cholera epidemic [11], choas behaviour [12], prediction of desertification by global warming [13] and many more. Now it's connected more with common applications. Understanding differential equations and the analytical and numerical solutions which describe these models is needed because of the nature of the nonlinear problems that arise in these various disciplines. As it is essential for properly simulating the behaviour of complex systems, the results presented above show how important FC is for modern scientific research and applications.

The use of FC to model influenza and to account for the effects of memory and non-locality in the dynamics of epidemics constitutes the main objectives of this study. This method is able to produce more accurate and comprehensive epidemiology models for influenza, informing public health policy and decision-making [14]. Gilberto et al. to describe and interpret influenza outbreaks. The suggestion of a nonlinear FO model was made in [15]. Using FO in the model yielded numerical results that closely mimic those from population-level influenza data. The numerical simulations for FO nonlinear mathematical model of influenza was provided by Zulqurnain et al. [16]. There have been some researchers presented for obtaining more accurate performances than the integer order. For the dynamical spread of the avaian influenza virus sentenced Xingyang and Chuanju [17] design a nonlinear FO epidemic model. Through simulations, they found that the solution of the FO model approaches a stationary state as the fractional derivative value diminishes over time. According to Abdoon et al., the output of the

FO model was closer to some of the real data than was the integer-order model. [18], who explored the response of influenza-positive approaches to real data. This further highlights how vital FC is for evaluating risks for these epidemics.

The literature previously discussed different approaches for solving these models. Some methods proposed recently are the homotopy analyis method (HAM) introduced by Liao Shijun in 1992 [19], which has been applied to a number of challenges in science and technology. The homotopy of the HAM gradually contorts a tentative mimic of the exact solution to the problem at hand. The $q-$homotopy analysis transform technique ($q-$HATM) is an advanced method combining the Laplace transform (LT) with $q-$HAM; it was first introduced by Singh et al. [20]. It may introduce a useful feature for epidemic problem awareness, which is the memory effect with FO. The $q-$HATM and Predictor-Corrector (PC) approach are crucial for solving the FO SIR model due to its effectiveness, versatility, and precision. We initially included the semi-analytical method known as $q-$HATM into the existing framework to offer a hybrid approach that ensures quick convergence and adaptability while working with nonlinear components. In order to better comprehend the dynamics of the model, we also employed the PC method. Recent investigations [21] have proven the PC approach's versatility and consistency across a variety of models. These methods are therefore very useful since they do not require any assumptions, discretization, or major simplifications, which makes them a reliable way to examine complex systems. Additionally, with sufficient numeric support for the random iterational modifications, it stabilizes the resultant output. The presence of them allows for overall validation which also reduce computing arrors and maintains a high precision. These techniques enhance computing efficiency and appropriate to simulate the inticate dynamics of influenza transmission, in addition to providing reliable information for public health planning and predictions of epidemics.. Further related studies can be found in [22, 23, 24, 25, 26].

This paper appears in the following format: Essential definitions of the FC and LT are furnished in Section 2. A thorough formulation and description of the model in dispute is given in Section 3. In Section 4, we presented the $q-$HATM method as a means of analysing the solutions of the model under consideration and provided illustrations for the convergence and uniqueness analyses. Section 5 presents the solutions and their graphical representation with the

aid of the $q-$HATM technique. The model's PC approach solution is shown in Section 6. The obtained results and graphs have been discussed for considered problems in Section 7. Lastly, Section 8 reports on our work's conclusions.

2. PRELIMINARIES

Following are the fundamental definitions of FC and LT that need to be properly included in the existing work.

Definition 1. *The definition of the fractional integral for the function $g(t) \in C_{-1}^{\ell}$ with regard to the Riemann-Liouville* [2, 3] *of order δ is*

$$J^{\delta} g(t) = \frac{1}{\Gamma(\delta)} \int_0^t (t-\theta)^{\delta-1} g(\theta)\, d\theta, \;\; t > 0, \delta > 0, \tag{1}$$

$$J^0 g(t) = g(t).$$

Definition 2. [4, 5] *defines the CFD for the function $g(t) \in C_{-1}^{\ell}$ as*

$${}_0D_t^{\delta} g(t) = \begin{cases} \frac{d^{\ell} g(t)}{dt^{\ell}}, & \delta = \ell \in \mathbb{N}, \\ \frac{1}{\Gamma(\ell - \delta)} \int_0^t (t-\theta)^{\ell-\delta-1} g^{(\ell)}(\theta)\, d\theta, & \delta \in (\ell-1, \ell),\ \ell \in \mathbb{N}. \end{cases} \tag{2}$$

Definition 3. *Let the LT of $g(t)$ be $L\big[g(t)\big] = \int_0^{\infty} e^{-st} g(t)\, dt$. Then, the LT of $g(t)$ in Caputo sense* [3, 4, 5] *is demarcated as*

$$L\big[D_t^{\delta} g(t)\big] = s^t G(s) - \sum_{k=0}^{\ell-1} s^{\delta-k-1} g^{(k)}\left(0^+\right), \quad \ell - 1 < \delta \leq \ell, \tag{3}$$

where $G(s)$ signifies the LT of $g(t)$.

3. MODEL FORMULATION

By creating mathematical models and examining their dynamical behaviours, it is a significant and useful method for understanding epidemic problems. Three nonlinear differential equations make up the SIR epidemic model of influenza, which we take into consideration in our work. Three groups make up the total population N of a given region at any given time: susceptible individuals, infected individuals and removed individuals (S, I, R). The influenza SIR model is given in Figure 1.

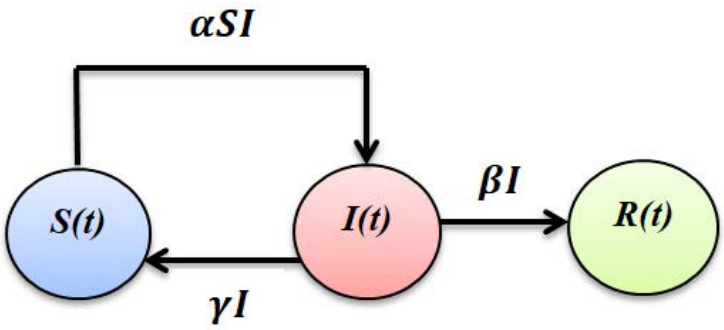

FIGURE 1. Schematic representation of the compartmental flow diagram for the influenza SIR model.

Permit the disease to spread at a rate of α to someone who is susceptible and at a rate of β and γ to an infected person respectively, by contact with removed and susceptible individuals. The mathematical model of integer-order that has been presented is expressed as follows [14]:

$$\begin{aligned} \frac{dS}{dt} &= -\alpha SI + \gamma I, \\ \frac{dI}{dt} &= \alpha SI - (\gamma+\beta)I, \\ \frac{dR}{dt} &= \beta I. \end{aligned} \tag{4}$$

The infection, elimination, and recovery rates are represented by the positive constants α, β and γ, respectively. We choose the CFD due to its linear property, and it is more suitable for modeling real-world problems with initial conditions where the value of the function and its derivatives are specified at a single point, and it is bounded. Therefore, we modify the system above to incorporate the impact of non-locality by replacing the CFD of the following form for the time derivative:

$$\begin{aligned} {}^{C}D_t^{\eta} S(t) &= -\alpha SI + \gamma I, \\ {}^{C}D_t^{\eta} I(T) &= \alpha SI - (\gamma+\beta)I, \qquad 0 < \eta \leq 1 \\ {}^{C}D_t^{\eta} R(t) &= \beta I, \end{aligned} \tag{5}$$

with initial settings

$$S(0) = a_0,\ I(0) = b_0,\ R(0) = c_0. \tag{6}$$

4. THE CORE CONCEPT OF $q-$HATM

The partial differential equation of FO that is both nonlinear and nonhomogeneous will be examined to introduce the basic theory of the proposed methodology:

$$D_t^{\eta} z(\vartheta,t) + Rz(\vartheta,t) + Nz(\vartheta,t) = f(\vartheta,t),\ \ n-1 < \eta \leq n, \tag{7}$$

where $f(\vartheta,t)$ is the source term, the linear and nonlinear differential operators are denoted by R and N respectively and the CFD of the function $z(\vartheta,t)$ is $D_t^{\eta} z(\vartheta,t)$. This CFD is preferred in many physical applications due to its better handling of initial conditions and its consistency with the properties of standard integer-order derivatives, while the Riemann-Liouville, Grunwald-Letnikov, and other fractional derivatives are more commonly used in the mathematical theory of FC. The CFD gives smoother behaviour compared to some other fractional derivatives. This smoothness property is desirable as it leads to more continuous and physically realistic models. Using the LT on Equation 7, we now obtain

$$s^{\eta} L[z(\vartheta,t)] - \sum_{r=0}^{n-1} s^{\eta-r-1} z^{(r)}(\vartheta,t) + L[Rz(\vartheta,t)] + L[Nz(\vartheta,t)] = L[f(\vartheta,t)]. \tag{8}$$

After reducing Equation 8, we obtain

$$L[z(\vartheta,t)] - \frac{1}{s^{\eta}} \sum_{r=0}^{n-1} s^{\eta-r-1} z^{(r)}(\vartheta,0) + \frac{1}{s^{\eta}} \{L[Rz(\vartheta,t) + Nz(\vartheta,t) - f(\vartheta,t)]\} = 0. \tag{9}$$

For the nonlinear operator, the homotopy analysis approach defines it as

$$N[\phi] = L[\phi] - \tfrac{1}{s^{\eta}} \textstyle\sum_{r=0}^{n-1} s^{\eta-r-1} \phi^{(r)}(0^+) + \tfrac{1}{s^{\eta}} \{L[R\phi] + L[N\phi] - L[f]\}, \tag{10}$$

where $\phi(\vartheta,t;q)$ is real function of ϑ, t and q and $q \in \left[0, \frac{1}{n}\right]$ $(n \geq 1)$.
In the following manner, we construct a homotopy for an auxiliary function that is non-zero:

$$L[\phi(\vartheta,t;q) - z_0(\vartheta,t)](1-nq) = q\hbar N[\phi(\vartheta,t;q)], \tag{11}$$

where L stands for the LT, q is the embedding parameter, an auxiliary parameter is $\hbar \neq 0$, an unknown function is $\phi(\vartheta,t;q)$, and an initial approximation of $z(\vartheta,t)$ is $z_0(\vartheta,t)$. The outcomes that follow are valid for $q = 0$ as well as $q = \frac{1}{n}$:

$$\phi(\vartheta,t;0) = z_0(\vartheta,t),\ \ \phi\left(\vartheta,t;\frac{1}{n}\right) = z(\vartheta,t). \tag{12}$$

Therefore, the solution $\phi(\varsigma,t;q)$ converge from $z_0(\vartheta,t)$ to the real solution $z(\vartheta,t)$ by amplifying q in the interval $\left[0,\frac{1}{r}\right]$. By expanding the function ϕ in series form using the Taylor theorem near q, one can obtain

$$\phi(\vartheta,t;q) = z_0(\vartheta,t) + \sum_{\mu=1}^{\infty} z_\mu(\vartheta,t)\, q^\mu , \tag{13}$$

where

$$z_\mu(\vartheta,t) = \frac{1}{\mu!}\left(\frac{\partial^\mu \phi(\vartheta,t;q)}{\partial q^\mu}|_{\mathrm{q}=0}\right). \tag{14}$$

The series Equation 13 converges at $q=\frac{1}{n}$ with choice of the auxiliary linear operator, n, $\hbar$ and the initial approximation $z_0(\vartheta,t)$. It results in one of the non-linear equation's original solutions, which is of the following form:

$$z(\vartheta,t) = z_0(\vartheta,t) + \sum_{\mu=1}^{\infty} z_\mu(\vartheta,t)\left(\frac{1}{n}\right)^\mu . \tag{15}$$

By differentiating Equation 11 μ-times with regards to embedding parameter, dividing that equation by $\mu!$ and finally taking $q=0$, we can get μ^{th} order deformation equation as

$$L[z_\mu(\vartheta,t) - k_\mu z_{\mu-1}(\vartheta,t)] = \hbar H(\vartheta,t) R_\mu(\vec{z}_{\mu-1}), \tag{16}$$

where the following is how the vectors are defined

$$\vec{z}_\mu(\vartheta,t) = \{z_0, z_1, \ldots, z_\mu\}. \tag{17}$$

The inverse LT is applied to Equation 16 to yield the recursive equation that follows

$$z_\mu(\vartheta,t) = k_\mu z_{\mu-1}(\vartheta,t) + \hbar L^{-1}[H(\vartheta,t) R_\mu(\vec{z}_{\mu-1})], \tag{18}$$

where

$$\begin{aligned} R_\mu(\vec{z}_{\mu-1}) = {} & L\left[z_{\mu-1}(\vartheta,t)\right] - \left(1-\tfrac{k_\mu}{n}\right)\left(\textstyle\sum_{r=0}^{n-1} s^{\eta-r-1} z^{(r)}(\vartheta,0) + \tfrac{1}{s^\eta} L\left[f(\vartheta,t)\right]\right) \\ & + \tfrac{1}{s^\eta} L\left[R z_{\mu-1} + H_{\mu-1}\right], \end{aligned} \tag{19}$$

and

$$k_\mu = \begin{cases} 0, & \mu \le 1, \\ n, & \mu > 1. \end{cases} \tag{20}$$

The homotopy polynomial H_μ in Equation 19 is defined as

$$H_\mu = \frac{1}{\mu!}\left[\frac{\partial^{\mu-1}\phi(\vartheta,t;q)}{\partial q^\mu}\right]_{\mathrm{q}=0} \text{ and } \phi(\vartheta,t;q) = \phi_0 + \phi_1 q + \phi_2 q^2 + ... \tag{21}$$

By Equation 18 and Equation 19, we have

(22)

$$\begin{aligned} z_\mu(\vartheta,t) = {} & \left(k_\mu + \hbar\right) z_{\mu-1}(\vartheta,t) - \left(1 - \tfrac{k_\mu}{n}\right) L^{-1}\left(\textstyle\sum_{r=0}^{n-1} s^{\eta-r-1} z^{(r)}(x,0) + \tfrac{1}{s^\eta} L\left[f(\vartheta,t)\right]\right) \\ & + \hbar L^{-1}\left\{\tfrac{1}{s^\eta} L\left[R\, z_{\mu-1} + H_{\mu-1}\right]\right\}. \end{aligned}$$

Ultimately, the iterative terms of $z_\mu(\vartheta,t)$ are obtained by solving Equation 22. Presenting the $q-$HATM series solution is

$$z(\vartheta,t) = \textstyle\sum_{\mu=0}^{\infty} z_\mu(\vartheta,t). \tag{23}$$

The convergence theorem and uniqueness are now interpreted for the projected model using the suggested methodology.

Theorem 4.1. *(Uniqueness theorem)*[27]
Using $q-$HATM, for every $\lambda \in (0,1)$ the non-linear FDE Equation 13 has a unique solution, where $\lambda = (\hbar + n) + T(\omega + \varepsilon)\hbar$.

Theorem 4.2. *(Convergence theorem)* [27]
Let $H : \mathrm{X} \to \mathrm{X}$ be a non-linear mapping and let X *be a Banach space. In light of Banach fixed point theory, if we assume that*

$$\|H(z) - H(w)\| \leq \lambda \|z - w\|, \ \forall\, z, w \in \mathrm{X} \tag{24}$$

then H has a fixed point. For an arbitrary choice of $z_0, w_0 \in \mathrm{X}$, the $q-$HATM obtained sequence likewise converges to a fixed point of H and

$$\left\|z_\mu - z_n\right\| \leq \frac{\lambda^n}{1-\lambda}\|z_1 - z_0\|. \tag{25}$$

5. $q-$HATM Solution for Considered Influenza SIR Epidemic Model

This section presents solutions for various parameter values in the model Equation 5 and demonstrates that these solutions match the qualitative aspects of the solutions. Consider time-fractional equations for the SIR epidemic model of influenza

$$
\begin{aligned}
&{}^{C}D_t^{\eta} S(t) = -\alpha SI + \gamma I, \\
&{}^{C}D_t^{\eta} I(t) = \alpha SI - \gamma I - \beta I, \qquad 0 < \eta \leq 1 \\
&{}^{C}D_t^{\eta} R(t) = \beta I.
\end{aligned} \tag{26}
$$

regarding initial conditions

$$
S(0) = a_0,\ I(0) = b_0,\ R(0) = c_0. \tag{27}
$$

Using the conditions given in Equation 27 and LT applied to the system of Equation 26 we now have

$$
\begin{aligned}
&L[S(t)] - \tfrac{1}{s}(S(0)) + \tfrac{1}{s^{\eta}} L[\alpha SI - \gamma I] = 0, \\
&L[I(t)] - \tfrac{1}{s}(I(0)) + \tfrac{1}{s^{\eta}} L[-\alpha SI + \gamma I + \beta I] = 0, \\
&L[R(t)] - \tfrac{1}{s}(R(0)) + \tfrac{1}{s^{\eta}} L[-\beta I] = 0.
\end{aligned} \tag{28}
$$

The non-linear operator is now defined as follows

$$
\begin{aligned}
&N_1[\phi_1, \phi_2, \phi_3] = L[\phi_1] - \tfrac{1}{s}(a_0) + \tfrac{1}{s^{\eta}} L[\alpha\phi_1\phi_2 - \gamma\phi_2], \\
&N_2[\phi_1, \phi_2, \phi_3] = L[\phi_2] - \tfrac{1}{s}(b_0) + \tfrac{1}{s^{\eta}} L[-\alpha\phi_1\phi_2 + \gamma\phi_2 + \beta\phi_2], \\
&N_3[\phi_1, \phi_2, \phi_3] = L[\phi_3] - \tfrac{1}{s}(c_0) + \tfrac{1}{s^{\eta}} L[-\beta\phi_2].
\end{aligned} \tag{29}
$$

With the use of the proposed algorithm, the deformation equation of μ-th order can be obtained as

$$
\begin{aligned}
&L\left[S_{\mu}(t) - k_{\mu} S_{\mu-1}(t)\right] = \hbar \left\{ R_{1,\mu}\left[\vec{S}_{\mu-1}(t), \vec{I}_{\mu-1}(t), \vec{R}_{\mu-1}(t)\right] \right\}, \\
&L\left[I_{\mu}(t) - k_{\mu} I_{\mu-1}(t)\right] = \hbar \left\{ R_{2,\mu}\left[\vec{S}_{\mu-1}(t), \vec{I}_{\mu-1}(t), \vec{R}_{\mu-1}(t)\right] \right\}, \\
&L\left[R_{\mu}(t) - k_{\mu} R_{\mu-1}(t)\right] = \hbar \left\{ R_{3,\mu}\left[\vec{S}_{\mu-1}(t), \vec{I}_{\mu-1}(t), \vec{R}_{\mu-1}(t)\right] \right\},
\end{aligned} \tag{30}
$$

where

(31)

$$
\begin{aligned}
R_{1,\mu}\left[\vec{S}_{\mu-1}(t), \vec{I}_{\mu-1}(t), \vec{R}_{\mu-1}(t)\right] &= L\left[S_{\mu-1}(t)\right] - \left(1 - \tfrac{k_{\mu}}{n}\right) \tfrac{1}{s}(a_0) \\
&\quad + \tfrac{1}{s^{\eta}} L\left[\alpha \textstyle\sum_{i=0}^{\mu-1} S_i(t) I_{\mu-1-i}(t) - \gamma I_{\mu-1}(t)\right], \\
R_{2,\mu}\left[\vec{S}_{\mu-1}(t), \vec{I}_{\mu-1}(t), \vec{R}_{\mu-1}(t)\right] &= L\left[I_{\mu-1}(t)\right] - \left(1 - \tfrac{k_{\mu}}{n}\right) \tfrac{1}{s}(b_0) \\
&\quad + \tfrac{1}{s^{\eta}} L\left[-\alpha \textstyle\sum_{i=0}^{\mu-1} S_i(t) I_{\mu-1-i}(t) + \gamma I_{\mu-1}(t) + \beta I_{\mu-1}(t)\right], \\
R_{3,\mu}\left[\vec{S}_{\mu-1}(t), \vec{I}_{\mu-1}(t), \vec{R}_{\mu-1}(t)\right] &= L\left[R_{\mu-1}(t)\right] - \left(1 - \tfrac{k_{\mu}}{n}\right) \tfrac{1}{s}(c_0) + \tfrac{1}{s^{\eta}} L\left[-\beta I_{\mu-1}(t)\right].
\end{aligned}
$$

Performing the inverse LT on the system of Equation 30, we obtain

$$\begin{aligned} S_\mu(t) &= k_\mu S_{\mu-1}(t) + \hbar L^{-1}\left[R_{1,\mu}\right], \\ I_\mu(t) &= k_\mu I_{\mu-1}(t) + \hbar L^{-1}\left[R_{2,\mu}\right], \\ R_\mu(t) &= k_\mu R_{\mu-1}(t) + \hbar L^{-1}\left[R_{3,\mu}\right]. \end{aligned} \tag{32}$$

When employing the initial conditions to solve the aforementioned system of equations $S(0) = a_0 = 620$, $I(0) = b_0 = 10$, $R(0) = c_0 = 70$, we have

$$\begin{aligned} &S_0(t) = 620, \\ &I_0(t) = 10, \\ &R_0(t) = 70, \\ &S_1(t) = \tfrac{6.15\hbar t^\eta}{\Gamma[\eta+1]}, \\ &I_1(t) = \tfrac{-5.43\hbar t^\eta}{\Gamma[\eta+1]}, \\ &R_1(t) = \tfrac{-0.72\hbar t^\eta}{\Gamma[\eta+1]}, \\ &S_2(t) = (n+\hbar)\tfrac{6.15\hbar t^\eta}{\Gamma[\eta+1]} - \tfrac{3.27795\hbar^2 t^{2\eta}}{\Gamma[2\eta+1]}, \\ &I_2(t) = (n+\hbar)\tfrac{-5.43\hbar t^\eta}{\Gamma[\eta+1]} + \tfrac{2.886995\hbar^2 t^{2\eta}}{\Gamma[2\eta+1]}, \\ &R_2(t) = (n+\hbar)\tfrac{-0.72\hbar t^\eta}{\Gamma[\eta+1]} + \tfrac{0.39096\hbar^2 t^{2\eta}}{\Gamma[2\eta+1]}, \\ &\vdots \end{aligned}$$

It is possible to retrieve the remaining iterative terms in this manner. Thus, the system of Equation 26 in the $q-$HATM series has a solution given by

$$\begin{aligned} S(t) &= S_0(t) + \textstyle\sum_{\mu=1}^{\infty} S_\mu(t)\left(\frac{1}{n}\right)^\mu, \\ I(t) &= I_0(t) + \textstyle\sum_{\mu=1}^{\infty} I_\mu(t)\left(\frac{1}{n}\right)^\mu, \\ R(t) &= R_0(t) + \textstyle\sum_{\mu=1}^{\infty} R_\mu(t)\left(\frac{1}{n}\right)^\mu. \end{aligned} \tag{33}$$

Here, we considered the influenza arbitrary-order SIR epidemic model with primary cases $S(0) = 620$, $I(0) = 10$ and $R(0) = 70$ and the value pf parameters are $\alpha = 0.001$, $\beta = 0.072$ and $\gamma = 0.005$. Figure 2 displays the 3D graphs of the obtained solutions for S, I, and R with respect to t. Figure 3 displays the $\hbar$-curves for the framework considered in Equation 26 at different η values. Figure 4 explores the nature of the solutions found with changes in time t for different values of η.

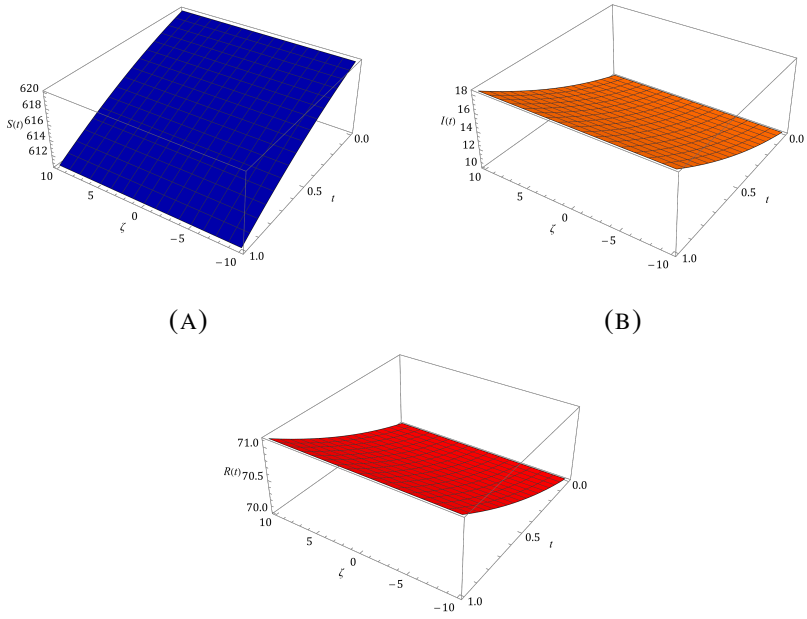

(A) (B)

(C)

FIGURE 2. Behaviour of $q-$HATM solution Equation 33 for $S(t)$, $I(t)$ and $R(t)$ on the subject of $\hbar = -1$ and $n = 1$ is presented in 3D graphs.

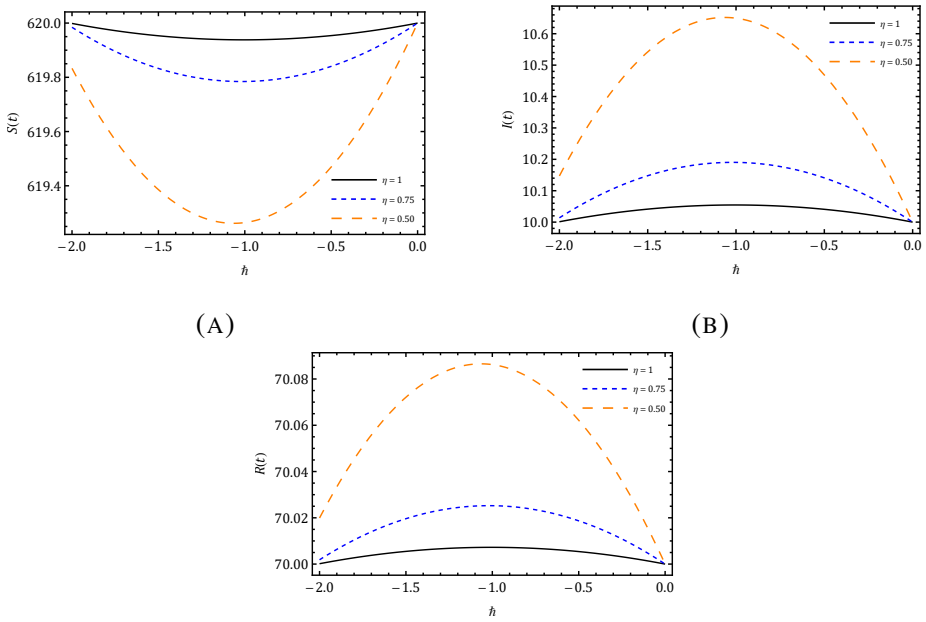

(A) (B)

(C)

FIGURE 3. $\hbar-$ curves are plotted for the gained solution with diverse values of η.

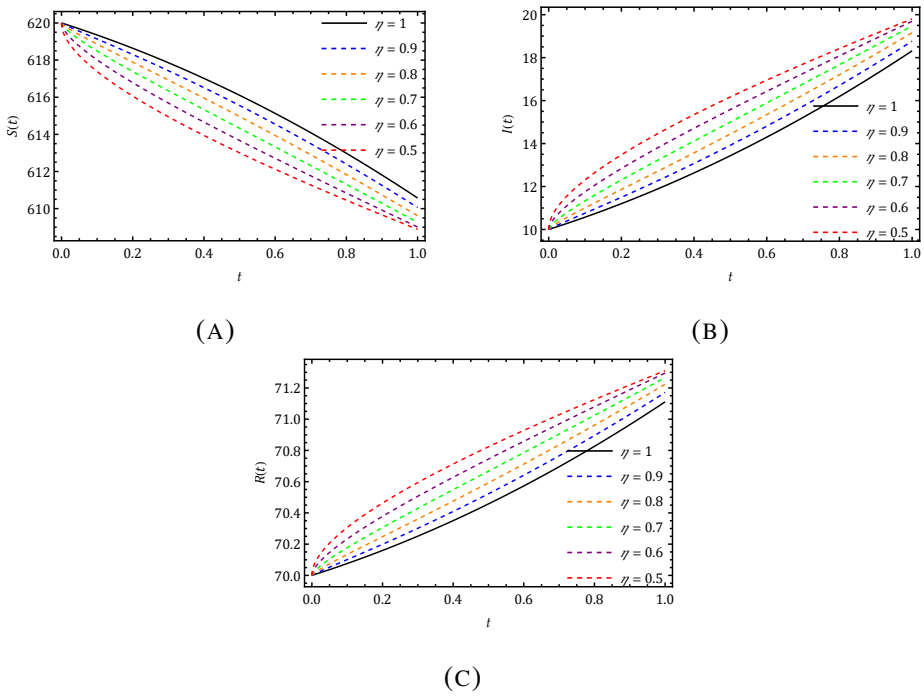

FIGURE 4. Response of solutions $S(t)$, $I(t)$, $R(t)$ by $q-$HATM with regard to t with varying η values are plotted.

The model under study is certainly dependent on the time-fractional order derivative, as shown by Table 1-Table 3. We also present the comparative numerical solutions derived by RK4, RPS technique, and $q-$HATM.

TABLE 1. Approximate value of $S(t)$ using $q-$HATM and compared with Runge-Kutta Fourth Order (RK4) method and Residual Power Series (RPS) method for $\eta = 1$.

t	RK4 solution [14]	RPS solution [14]	q-HATM solution
0.1	619.368327701129830	619.368327657510350	619.352220500
0.2	618.702153816378770	618.702153724652930	618.638882000
0.3	617.999682039910570	617.999681895280220	617.859984500
0.4	617.259032603941480	617.259032401282640	617.015528000
0.5	616.478239561945540	616.478239295794650	616.105512499
0.6	615.655248125904110	615.655247790443130	615.129937999
0.7	614.787912080138200	614.787911669181200	614.088804500
0.8	613.873991297021010	613.873990803999960	612.982112000
0.9	612.911149382834760	612.911148800787370	611.809860500
1.0	611.896951485213090	611.896950806769950	610.572050000

TABLE 2. $I(t)$'s approximate value using $q-$HATM for $\eta = 1$ and compared with RK4 and RPS method.

t	RK4 solution [14]	RPS solution [14]	q-HATM solution
0.1	10.557682415377140	10.557682454124135	10.571869900
0.2	11.145742665297318	11.145742746766953	11.201479600
0.3	11.765752718571312	11.765752847013921	11.888829099
0.4	12.419356430322715	12.419356610275818	12.633918400
0.5	13.108271733277171	13.108271969577906	13.436747500
0.6	13.834292759467655	13.834293057265034	14.297316400
0.7	14.599291870396474	14.599292235163372	15.215625100
0.8	14.599291870396474	15.405222008647254	16.191673599
0.9	16.254116280801693	16.254116797279011	17.225461900
1.0	17.148093929799238	17.148094531720652	18.316990000

TABLE 3. Approximate value of $R(t)$ by $q-$HATM with comparition of RK4 and RPS method for $\eta = 1$.

t	RK4 solution [14]	RPS solution [14]	q-HATM solution
0.1	70.073989883493013	70.073989888365404	70.07590960
0.2	70.152103518323841	70.152103528579929	70.15963840
0.3	70.234565241518069	70.234565257705697	70.25118640
0.4	70.321610965735758	70.321610988441307	70.35055360
0.5	70.413488704777279	70.413488734627379	70.45774000
0.6	70.510459114628276	70.510459152291887	70.57274560
0.7	70.612796049465331	70.612796095655639	70.69557040
0.8	70.720787131876406	70.720787187352826	70.82621440
0.9	70.834734336363510	70.834734401933645	70.96467760
1.0	70.954954584987661	70.954954661509220	71.11096000

6. SOLUTION OF THE CONSIDERED SIR EPIDEMIC MODEL OF INFLUENZA USING PC ALGORITHM

We will now go into the developed version of the classical trapezoidal rule, known as the PC technique. Several instances of practical implementations have demonstrated the effectiveness of this strategy. Here, we use the PC technique [21] to get the solution of the predicted model.

Examine the differential equation model of the FO influenza SIR outbreak

$$ {}^{C}D_t^{\eta}\left[S(t)\right] = \mathrm{X}_1(t,S),\ \ 0<\eta\leq 1,\ \ t\in[0,T]\,, \tag{34} $$

$$ S(t) = a. \tag{35} $$

Let's design a grid that is consistent, $\{t_k = kh : k = -m,\ -m+1\,,\ -m+2,\ldots,0\,,\ldots,\mathbb{N}\}$ and $\mathbb{N}h = T$, where m are integers and $\mathbb{N}$ denotes the collection of natural number.

$$ S_h(t_i) = a,\ i = -m,\ -m+1,\ -m+2\ldots,\ -2,\ -1,\ 0. \tag{36} $$

With reference to Equation 34 and Equation 35, we would like to evaluate $S_h(t_{k+1})$ making use of the Volterra integral equation and $S_h(t_i)\approx S(t_i),\ (i=-m,-m+1,-m+2\ldots,-1,0,1,\ldots,k)$. Under the assumption that the approximations have already been computed.

$$ S(t_{k+1}) = S(0) + \frac{1}{\Gamma(\eta)}\int_0^{t_{k+1}} (t_{k+1}-\xi)^{\eta-1}\mathrm{X}_1(\xi,S(\xi))d\xi. \tag{37} $$

We use approximations $S_h(t_k)$ for $S(t_k)$ in Equation 37. Additionally, the product trapezoidal quadrature formula in Equation 37 is used to get the integral. So, the formula for the corrector is

$$ S_h(t_{k+1}) \;=\; S(0) \;+\; \frac{h^{\eta}}{\Gamma(2+\eta)}\,\mathrm{X}_1(t_{k+1},S_h(t_{k+1})) + \frac{h^{\eta}}{\Gamma(2+\eta)}\sum_{i=0}^{k} l_{i,k+1}\,\mathrm{X}_1(t_i,S_h(t_i)), \tag{38} $$

where

$$ l_{i,k+1} = \begin{cases} k^{1+\eta}-(1+k)^{\eta}(k-\eta), & i=0 \\ (k+2-i)^{1+\eta}+(k-i)^{1+\eta}-2\,(k+1-i)^{1+\eta},\ 1\leqslant i\leqslant k \\ 1\,, & i=k+1. \end{cases} \tag{39} $$

Equation 38 has the unknown $S_h(t_{k+1})$ component on both sides. The nonlinearity of X_1 prevents an explicit solution to Equation 38 for $S_h(t_{k+1})$. As a result, we substitute an estimate

$S_h^p(t_{k+1})$, also referred to as the predictor, for the $S_h(t_{k+1})$ term on the right. The predictor term in Equation 38 is evaluated using the product rectangle rule.

$$S_h^p(t_{k+1}) = S(0) + \frac{1}{\Gamma(\eta)} \sum_{i=0}^{k} j_{i,k+1} \mathrm{X}_1(t_i, S_h(t_i)). \tag{40}$$

Here

$$j_{i,k+1} = \frac{h^\eta}{\eta}((k+1-i)^\eta - (k-i)^\eta). \tag{41}$$

Based on the calculations performed earlier, the corrector formulas for the remaining system of Equation 4 are as follows:

$$\begin{aligned} I_h(t_{k+1}) &= I(0) + \frac{h^\eta}{\Gamma(2+\eta)} \mathrm{X}_2(t_{k+1}, I_h(t_{k+1})) + \frac{h^\eta}{\Gamma(2+\eta)} \sum_{i=0}^{k} l_{i,k+1} \mathrm{X}_2(t_i, I_h(t_i)), \\ R_h(t_{k+1}) &= R(0) + \frac{h^\eta}{\Gamma(2+\eta)} \mathrm{X}_3(t_{k+1}, R_h(t_{k+1})) + \frac{h^\eta}{\Gamma(2+\eta)} \sum_{i=0}^{k} l_{i,k+1} \mathrm{X}_3(t_i, R_h(t_i)). \end{aligned} \tag{42}$$

Likewise, the predictor variables can be compute as follows

$$\begin{aligned} I_h^p(t_{k+1}) &= I(0) + \frac{1}{\Gamma(\eta)} \sum_{i=0}^{k} j_{i,k+1} \mathrm{X}_2(t_i, I_h(t_i)), \\ R_h^p(t_{k+1}) &= R(0) + \frac{1}{\Gamma(\eta)} \sum_{i=0}^{k} j_{i,k+1} \mathrm{X}_3(t_i, R_h(t_i)). \end{aligned} \tag{43}$$

Figure 5 displays the kind of outcomes that the PC approach achieved in relation to time for different FO values. The $q-$HATM and PC technique findings are displayed in Figure 6. The accuracy of the $q-$HATM approach is validated by the close agreement between the combined solution graphs produced by these two techniques. By comparing the semi-analytical approach with a conventional numerical solution, this comparison validates its dependability and improves confidence in its use for resolving nonlinear differential equations.

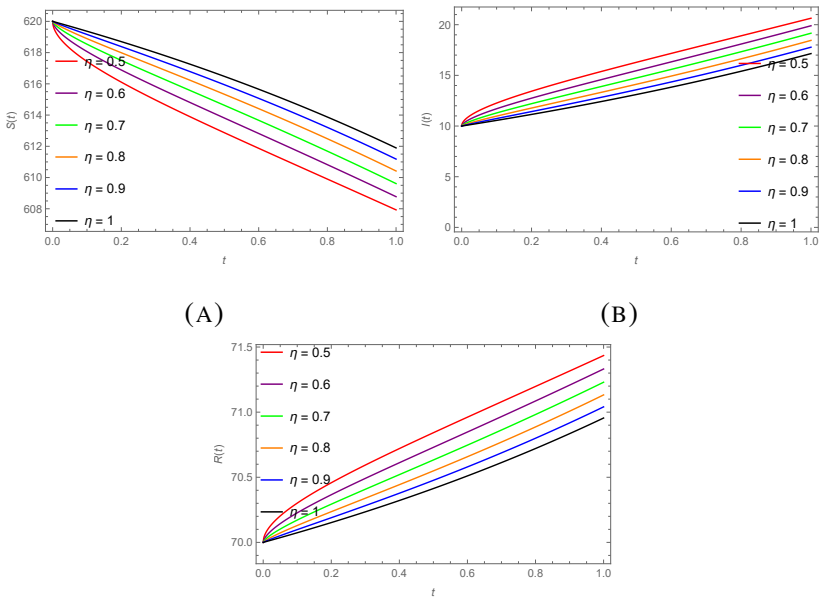

FIGURE 5. Plots for the solutions $S(t)$, $I(t)$ and $R(t)$ with time t for different FO (η) using PC approach.

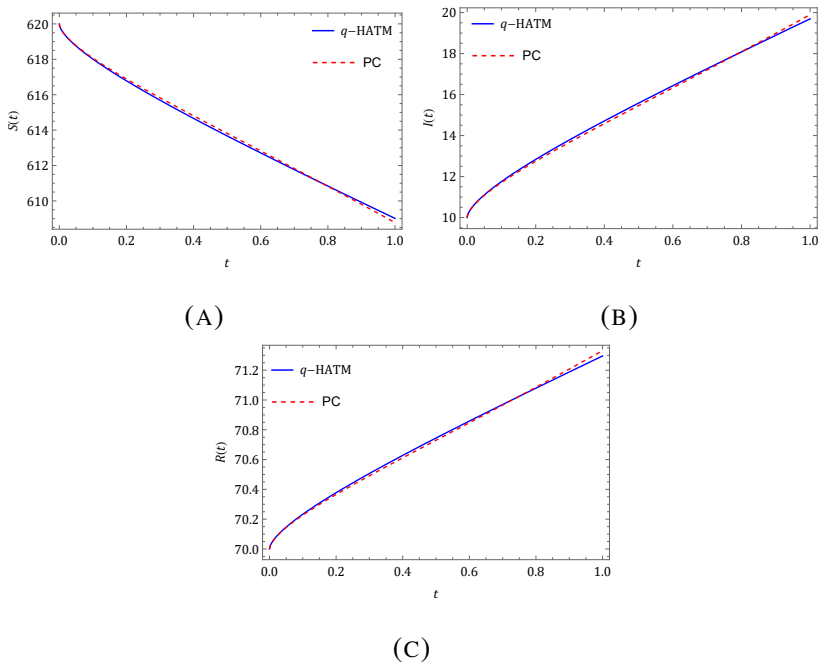

FIGURE 6. Plots of the solutions for $S(t)$, $I(t)$ and $R(t)$ achieved by the $q-$HATM and PC method.

7. Results and Discussion

Using numerical simulation and graphical representation, the proposed section's primary objective is to display susceptible, infected, and removed individuals of the arbitrary-order influenza SIR epidemic model. Additionally, we used the $q-$HATM and PC techniques to observe the behaviours of S, I and R with time t.

To verify that the suggested method is accurate and reliable, $q-$HATM has been used to evaluate the estimated analytical solutions. Table 1-Table 3 demonstrate how the model under consideration is obviously dependent on the time-fractional order derivative and also shows the comparative numerical solutions obtained by RK4, RPS method and $q-$HATM. So that the suggested method more successfully identifies susceptible, infected, and removed individuals than the RK4 and RPS methods. Therefore, the preferred approach is highly effective and systematic. This helps us to comprehend how the influenza SIR model behaves. The 3D graphs of the obtained solutions for S, I and R with regard to t are shown in Figure 2, which also shows an increase in recovered and infected persons and a decrease in susceptible individuals. The response of the solutions produced by the suggested algorithm for S, I and R for the value of the homotopy convergence control parameter $\hbar$ is shown in Figure 3. Here are the $\hbar$-curves for the framework taken into consideration in Equation 26 at various η values. When $\hbar$ is set appropriately, series solutions converge quickly. Additionally, this aids in the management and modification of the derived series solution's region of convergence. The nature of the solutions obtained for the considered SIR model with changes in time t for distinct values of η is explored in Figure 4, and these outcomes make it evident that the influenza model with arbitrary order is more adaptable.

We performed graphical simulations for the PC method solutions of the obtained Equation 40-Equation 43 using Mathematica and the numerical data. The nature of the outcomes provided by the proposed solution technique in relation to time for various FO values is shown in Figure 5. Therefore, by employing this method, we can comprehend the model's behavior with easily. Our solutions matched the results that the $q-$HATM achieved. Figure 6 shows the results of the $q-$HATM and PC method. We can see from Figure 6 that both strategies work well for the model under consideration.

8. Conclusion

The current framework looked into the $q-$HATM and PC methods solutions for the model under consideration. The model's fractional equations are of the Caputo sense. It becomes clear that we have achieved consistency with a more realistic and capable model when we take into account the CFD. A quickly convergent series form comprising the acquired $q-$HATM solutions is presented. We compute the numerical results and graphical representations of the two proposed approaches to verify their efficacy, and they show great agreement with the results reported in the publication of Meena and Kumar [14]. This implies that our fractional model is accurate, well-posed, and efficient. Examples that show how the fractional derivative impacts the result and recommended techniques are provided in this study. Studying FO differential equations and using the techniques for complex dynamical system analysis can be quite beneficial for many different fields. Additionally, FC offers up novel possibilities for mathematical modelling. Future research can study the stochastic effects, which can provide a more realistic representation of influenza spread. Its application will be further enhanced by expanding the model to incorporate real-time data assimilation, vaccination techniques, and multiple strains. Furthermore, the model's efficacy may be confirmed by applying it to actual influenza outbreaks using data particular to a certain region. This will help direct public health initiatives to better epidemic control.

Conflict of Interests

The authors declare that there is no conflict of interests.

References

[1] World Health Organization, Influenza (Seasonal), Accessed: Sep. 11, 2024. https://www.who.int/news-room/fact-sheets/detail/influenza-(seasonal).

[2] K.S. Miller, B. Ross, An Introduction to the Fractional Calculus and Fractional Differential Equations, Wiley, 1993.

[3] I. Podlubny, Fractional Differential Equations, Academic Press, New York, 1999.

[4] M. Caputo, Elasticita e Dissipazione, Zanichelli, Bologna (1969).

[5] M. Caputo, Linear Models of Dissipation Whose Q Is Almost Frequency Independent–Ii, Geophys. J. Int. 13 (1967), 529–539. https://doi.org/10.1111/j.1365-246x.1967.tb02303.x.

[6] B. Ross, The Development of Fractional Calculus 1695–1900, Hist. Math. 4 (1977), 75–89. https://doi.org/10.1016/0315-0860(77)90039-8.

[7] J.M. Cruz–Duarte, J. Rosales–Garcia, C.R. Correa–Cely, A. Garcia–Perez, J.G. Avina–Cervantes, A Closed Form Expression for the Gaussian–based Caputo–fabrizio Fractional Derivative for Signal Processing Applications, Commun. Nonlinear Sci. Numer. Simul. 61 (2018), 138–148. https://doi.org/10.1016/j.cnsns.2018.01.020.

[8] J. Yu, Y. Feng, Group Classification of Time Fractional Black-Scholes Equation with Time-Dependent Coefficients, Fract. Calc. Appl. Anal. 27 (2024), 2335–2358. https://doi.org/10.1007/s13540-024-00339-4.

[9] D.K. Archana, D.G. Prakasha, P. Veeresha, K.S. Nisar, An Efficient Technique for One-Dimensional Fractional Diffusion Equation Model for Cancer Tumor, Comput. Model. Eng. Sci. 141 (2024), 1347–1363. https://doi.org/10.32604/cmes.2024.053916.

[10] X. Zhang, R. Liu, J. Ren, Q. Gui, Adaptive Fractional Image Enhancement Algorithm Based on Rough Set and Particle Swarm Optimization, Fractal Fract. 6 (2022), 100. https://doi.org/10.3390/fractalfract6020100.

[11] A.H. Ali, A. Ahmad, F. Abbas, E. Hincal, A. Ghaffar, B. Batiha, H.A. Neamah, Modeling the Behavior of a Generalized Cholera Epidemic Model with Asymptomatic Measures for Early Detection, PLOS ONE 20 (2025), e0319684. https://doi.org/10.1371/journal.pone.0319684.

[12] D. Baleanu, G. Wu, S. Zeng, Chaos Analysis and Asymptotic Stability of Generalized Caputo Fractional Differential Equations, Chaos Solitons Fractals 102 (2017), 99–105. https://doi.org/10.1016/j.chaos.2017.02.007.

[13] E. Hakeem, S. Jawad, A.H. Ali, M. Kallel, H.A. Neamah, How Mathematical Models Might Predict Desertification From Global Warming and Dust Pollutants, MethodsX 14 (2025), 103259. https://doi.org/10.1016/j.mex.2025.103259.

[14] R.K. Meena, S. Kumar, Solution of Fractional Order SIR Epidemic Model using Residual Power Series Method, Palest. J. Math. 11 (2022), 12–24.

[15] G. González-Parra, A.J. Arenas, B.M. Chen-Charpentier, A Fractional Order Epidemic Model for the Simulation of Outbreaks of Influenza A(h1n1), Math. Methods Appl. Sci. 37 (2013), 2218–2226. https://doi.org/10.1002/mma.2968.

[16] Z. Sabir, S. Ben Said, Q. Al-Mdallal, A Fractional Order Numerical Study for the Influenza Disease Mathematical Model, Alex. Eng. J. 65 (2023), 615–626. https://doi.org/10.1016/j.aej.2022.09.034.

[17] X. Ye, C. Xu, A Fractional Order Epidemic Model and Simulation for Avian Influenza Dynamics, Math. Methods Appl. Sci. 42 (2019), 4765–4779. https://doi.org/10.1002/mma.5690.

[18] M.A. Abdoon, R. Saadeh, M. Berir, F. EL Guma, M. ali, Analysis, Modeling and Simulation of a Fractional-Order Influenza Model, Alex. Eng. J. 74 (2023), 231–240. https://doi.org/10.1016/j.aej.2023.05.011.

[19] S. Liao, Homotopy Analysis Method and Its Applications in Mathematics, J. Basic Sci. Eng. 5 (1997), 111–125.

[20] J. Singh, D. Kumar, R. Swroop, Numerical Solution of Time- and Space-Fractional Coupled Burgers' Equations via Homotopy Algorithm, Alex. Eng. J. 55 (2016), 1753–1763. https://doi.org/10.1016/j.aej.2016.03.028.

[21] P. Kumar, V. Suat Erturk, The Analysis of a Time Delay Fractional Covid-19 Model via Caputo Type Fractional Derivative, Math. Methods Appl. Sci. 46 (2020), 7618–7631. https://doi.org/10.1002/mma.6935.

[22] A. Ali, S. Jawad, A.H. Ali, M. Winter, Stability Analysis for the Phytoplankton-Zooplankton Model with Depletion of Dissolved Oxygen and Strong Allee Effects, Results Eng. 22 (2024), 102190. https://doi.org/10.1016/j.rineng.2024.102190.

[23] F.S. Khan, M. Khalid, A.A. Al-moneef, A.H. Ali, O. Bazighifan, Freelance Model with Atangana–baleanu Caputo Fractional Derivative, Symmetry 14 (2022), 2424. https://doi.org/10.3390/sym14112424.

[24] F.K. Alalhareth, U. Atta, A.H. Ali, A. Ahmad, M.H. Alharbi, Analysis of Leptospirosis Transmission Dynamics with Environmental Effects and Bifurcation Using Fractional-Order Derivative, Alex. Eng. J. 80 (2023), 372–382. https://doi.org/10.1016/j.aej.2023.08.063.

[25] A. Raza, R. Ali, S.M. Eldin, S.H. Alfalqui, A.H. Ali, New Fractional Approach for Cmc and Water Based Hybrid Nanofluid with Slip Boundary Layer: Applications of Fractal Fractional Derivative, Case Stud. Therm. Eng. 49 (2023), 103280. https://doi.org/10.1016/j.csite.2023.103280.

[26] A.H. Ali, M. Amir, J.U. Rahman, A. Raza, G.E. Arif, Design of Morlet Wavelet Neural Networks for Solving the Nonlinear Van Der Pol–mathieu–duffing Oscillator Model, Computers 14 (2025), 14. https://doi.org/10.3390/computers14010014.

[27] D. Kumar, J. Singh, D. Baleanu, A New Analysis for Fractional Model of Regularized Long-wave Equation Arising in Ion Acoustic Plasma Waves, Math. Methods Appl. Sci. 40 (2017), 5642–5653. https://doi.org/10.1002/mma.4414.